Optimization of Low-Dose Pediatric Chest CT Examination: Pediatric Phantom Study

Dafa Miftahuddin,[1] Audiena Gelung Prayitno,[1] Aditya Prayugo Hariyanto,[1] Djuli Pontjowijono,[2] and Endarko[1]

[1]*Department of Physics, Institut Teknologi Sepuluh Nopember, Kampus ITS-Sukolilo Surabaya 600111, East Java, Indonesia*
[2]*2Department of Radiology, Simpang Lima Gumul Hospital, Kediri 64182, East Java, Indonesia*

Abstract: This study used a Pediatric Thoracic phantom developed in-house to optimize low-dose pediatric chest CT examinations based on organ-specific doses and image quality. Four low-dose protocols with low tube voltage (kV) and low tube current (mA), combined with Filtered Back Projection (FBP) and iterative reconstruction (IR), were investigated. The lung, heart, and spinal cord doses were measured using the LD-V1 Film. The evaluation of the spatial resolution and noise was considered. The low-kV protocol exposed an average dose 29.55% lower than the low mA, but the peak Noise Power Spectrum (NPS) was significantly higher. No significant differences were found in the Modulation Transfer Function (MTF) curve at standard, low-mA, or low-kV doses. The combination of low kV and FBP produces images with a higher spatial resolution. The combination of low mA and IR effectively reduces image noise, thereby improving low-contrast object detection.

Keywords: Low Dose; Modulation Transfer function (MTF); Noise Power Spectrum (NPS); Pediatric

*Corresponding author: endarko@physics.its.ac.id

http://dx.doi.org/10.12962/j24604682.v20i1.19814
2460-4682

I. INTRODUCTION

Computed Tomography (CT) provides a more detailed image quality, good diagnostic accuracy, and short acquisition time, thereby increasing the frequency of CT examinations worldwide. In 2020, registered CT scanner installations worldwide reached almost 30,000 CT scans, 374 of which are in Indonesia [1, 2]. Even though it has provided advances in modern medical practice, CT has the potential for patient health problems due to the increased risk of radiation doses that can cause significant carcinogenic effects. In pediatric patients, body tissues are smaller and have greater radiosensitivity [3].

To minimize the risk of high radiation exposure in pediatric patients, a low-dose CT protocol was developed. This protocol reduces the tube voltage or current below the standard value. A schematic review study showed that low kV reduces the CT dose by 60% [3]. Meanwhile, a low tube current (low mA) provided optimal dose reduction in a study of four low-dose levels based on computed tomography dose index volume (CTDIvol) [4]. In contrast, low doses cause a significant increase in image noise when reconstructed using standard algorithms such as filtered back projection (FBP) [5]. More advanced reconstructions such as iterative reconstruction (IR) provide image noise suppression, but degrade other image quality parameters [6].

Several previous studies referred to the CTDIvol value for dose analysis in low-dose CT [3, 4, 6] and used image quality phantoms for CT image quality analysis [5, 6]. TDIvol is calculated using a standard cylindrical phantom, thereby not providing the dose distribution and image quality in the patient [7]. Another problem with pediatric size variables is that they depend on age. This size difference affects dose reduction and the resulting image noise, making it a significant challenge in dose and image studies on low-dose CT [8]. Further analysis of the combination of acquisition parameters and reconstruction methods in low-dose CT protocols is needed, especially in multiage pediatric patients. Some hospitals focus on CT examinations of adult patients, so that dose survey data and image quality in pediatric patients are not easy to obtain [9].

In this study, an in-house Pediatric Thoracic phantom was used to directly measure the organ-specific dose and image quality of low-dose CT examinations. Four low-dose protocols with low tube voltage (kV) and low tube current (mA) combined with Filtered Back Projection (FBP) and iterative reconstruction (IR), were investigated. This study is crucial for providing accurate dosage information and improving image quality in alignment with actual clinical practices. Furthermore, optimization of low-dose chest CT examination protocols in pediatric cases has become more attainable.

II. METHODOLOGY

This study used a pediatric-specific chest phantom made of polylactic acid (PLA), which is referred to as registered patent No. P00202102195 [10]. The radiation dose was measured using a calibrated LD-V1 film dosimeter of size 2×2 cm^2 [11]. The study flow is shown in Fig. 1, with CT scanners from the manufacturers of GE Brilliance 16-Slice at Simpang Lima Gumul Hospital, Kediri, Indonesia.

Four low-dose CT examination protocols were adapted from the American Association of Physicists in Medicine (AAPM) documents by reducing the current tube and volt-

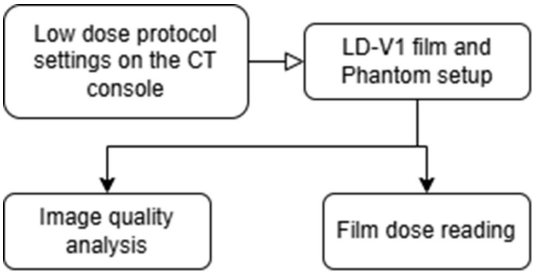

FIG. 1: Outline flow of a low-dose pediatric chest CT optimization study

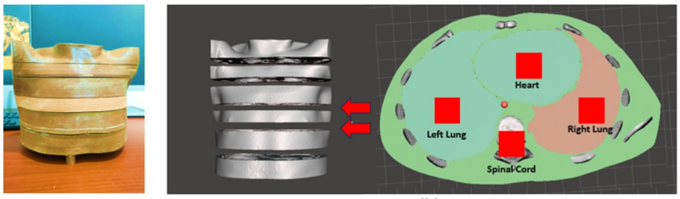

FIG. 2: (a) 4-year-old pediatric phantom made of PLA, (b) position of the dosimeter film on each organ.

age to a low dose (Fig.1) [11]. Image reconstruction is carried out with a standard algorithm: a filtered rear projection (FBP), and the Specific Iterative Reconstruction Algorithm (IR) uses fourth-generation hybrid iterative reconstruction (iDose4; level 3). The scanning parameters for all scanners are presented in Table I.

The measurement of organ-specific doses is important for determining the dose to pediatric organs. The film was placed in the right lung, left lung, spinal cord, and phantom heart (Fig. 2) and then scanned by CT scanners in each examination protocol. A different film was used for each protocol. The measurement of the focus dose on the mA (P1) protocol was low and low in kV (P3), in accordance with Table I. Radiation doses in the film were read with Epson Expression 10000 XL following a study by Tomic et al. [12].

For image quality, the spatial resolution of the image was evaluated using the MTF curve, while the characteristics of image noise were evaluated using the Noise Power Spectrum (NPS). The MTF curve is calculated from the edges of two materials with different contrast values, following previous research [13, 14]. The ROI was drawn on the edge of the right side and the heart to measure the pixel value of the two tissue edges (Fig. 3). The pixel value is averaged on the X-axis to create an Edge Spread Function (ESF) curve, the ESF is differentiated to create a Line Spread Function (LSF) curve, and the Fourier transformation from the LSF produces an MTF curve. The MTF curve was calculated automatically using IndoQCT [15]. The MTF curve and spatial frequency value of MTF10% were compared to each other.

Noise characterization is the most significant component of image-quality measurement. NPS provides a complete description of the noise texture rather than the standard deviation. NPS describes noise variations as a frequency function

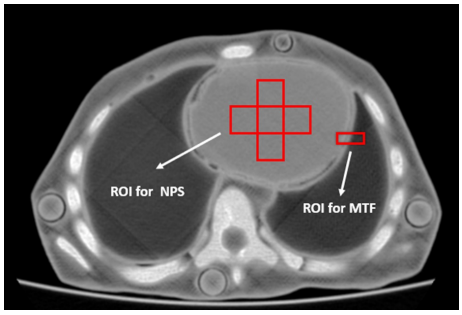

FIG. 3: ROI for computing Modulation Transfer Function (MTF) on the right lung edge and Noise Power Spectrum (NPS) on the heart.

[16]. NPS was calculated for the heart with a total ROI of 5, a size of 20 pixels (Fig. 3), and a sampling angle of 10. NPS was estimated using Eq. (1) [17]:

$$NPS_{x,y} = \frac{D_x D_y}{N_x N_y}[FFT(ROI_i(x,y)) - \overline{(\mathrm{ROI_i(x,y)})}]^2 \quad (1)$$

where D_x and D_y are pixels in mm, and N_x and N_y are the number of pixels in the x- and y-directions in the region of interest (ROI), respectively. $ROI_i(x,y)$ is the signal in the i-th ROI, ($(ROI_i$ (x,y)) is the mean of ROI_i(x, y). The region of interest (ROI) was automatically computed using indoQCT.

Statistical data analysis was performed using SPSS Statistics 25 with comparisons between groups using one-way analysis of variance (ANOVA). A 95% confidence interval (CI) was used, and a P value < 0.05 was considered statistically significant.

III. RESULTS AND DISCUSSIONS

A. Organ-Specific dose

Each irradiated LD-V1 film was scanned with an Epson Expression 10000 XL to read the radiation dose following a study by Tomic *et al.* [12]. The results are presented in Table II. The organ-specific dose measured with the film was higher than that indicated in the CTDIvol. The right and left lungs received a higher dose than the other organs did. The average radiation dose exposure to each organ was smaller when a low voltage was used. The protocol with low kV, on average, exposed a dose 29.55% lower than that with low mA.

B. Modulation Transfer Function (MTF)

In general, all MTF curves showed similar trends for all studied protocols (Fig. 4). FBP reconstruction at low mA and low kV produces spatial frequencies at MTF 0.1 (MTF10%) of 0.59 and 0.60 /mm, respectively, while IR at low mA and low kV produces MTF10% of 0.57 and 0.59 /mm, respectively.

TABLE I: Four protocols with variations in data acquisition and image reconstruction parameters.

Protocols	Low mA (P3) [CTDIvol = 1.40 mGy]		Low kV (P5) [CTDIvol = 1.40 mGy]	
	P1	P2	P3	P4
Tube Volatge (kV)	120	120	901 / 802	901 / 802
Tube Current (mA)	50	50	1201 / 1252	120 1/ 1252
Reconstruction	FBP	iDose (3)	FBP	iDose (3)
Acquisition mode	Helical	Helical	Helical	Helical
Gantry rotation Time (s)	0.5	0.5	0.5	0.5
Slice Thickness (mm)	3	3	3	3
Filed of View (mm)	250	250	250	250
Pitch	1	1	1	1
Matrix	512512	512512	512512	512512
Collimation (mm^2)	161.5	161.5	161.5	161.5

P = Protocols, CTDIvol = volume CT dose index

TABLE II: Average values of organ-specific absorbed dose at low mA (P1) and low kV (3).

Organ	Low mA (P1) [CTDIvol = 1.40 mGy]	Low mA (P1) [CTDIvol = 1.40 mGy]
Right Lung	2.91 0.50* mGy	2.29 0.20* mGy
Left Lung	2.59 0.40* mGy	2.17 0.66* mGy
Heart	2.05 0.21* mGy	1.39 0.23 mGy
Spinal Cord	1.98 0.31* mGy	1.02 0.10 mGy

*The radiation dose received by the organ is greater than the estimated CTDIvol dose

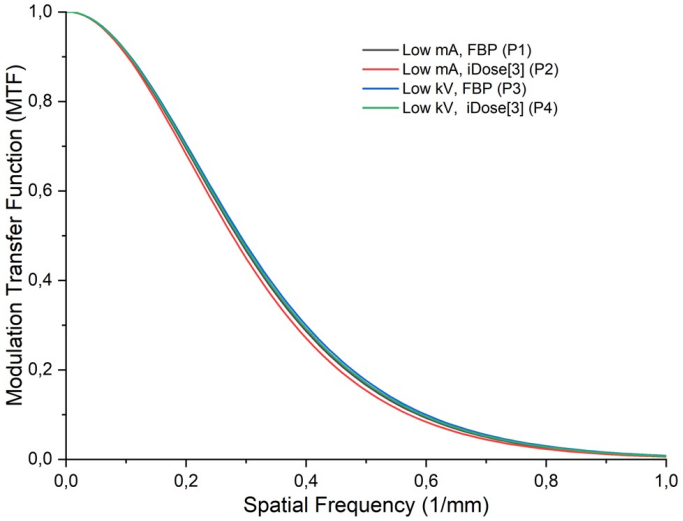

FIG. 4: MTF curves at low mA (P1, P2) and low kV (P3, P4) were set using the reconstructed images with FBP (P1, P3) and IR (P2, P4).

C. Noise Power Spectrum (NPS)

The noise characteristics of the CT images are described in the NPS curve. As shown in Fig. 5, the peak of the NPS

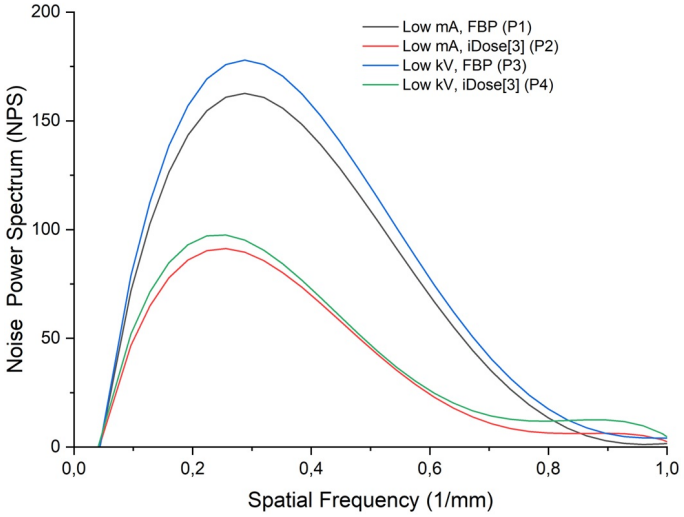

FIG. 5: NPS curves at low mA (P1, P2) and low kV (P3, P4) were set using the reconstructed images with FBP (P1, P3) and IR (P2, P4).

curve is much lower in the IR algorithm than in the FBP algorithm, both at low kV and low mA. Higher curve peaks indicate greater noise. IR significantly reduces the noise peaks in the image. When comparing low mA and low kV, low mA yields lower NPS peaks compared to low kV. These results are consistent when applying FBP and IR reconstruction

D. Discussion

A pediatric phantom was developed to study the dose and imaging in low-dose CT examinations. As shown in Table II, the organ-specific doses measured were higher than the CTDIvol values, except for the heart and spinal cord at low kV. The right and left lungs received higher doses in each protocol because the volume and position of these organs allow for high exposure. These results are similar to those of dose

studies using optically stimulated lighting (OSL) dosimeters [18]. CTDIvol was calculated using a 32 cm PMMA cylindrical phantom, in contrast to the axial section of the human body, which is generally elliptical [19]. Although the CTDIvol does not directly represent organ-specific doses, the use of low-dose protocols based solely on the CTDIvol may have unmeasured side effects. The higher the dose of radiation exposure to the patient's organs, the higher the risk to the patient's future.

In a comparison between protocols with low mA (P1) and low kV (P3), low kV provided an average dose exposure 29.55% lower than low mA in each organ. The tube voltage contributes to the energy of the electrons resulting from thermionic emissions to interact with the target and produce X-rays. The energy of an electron is directly proportional to the energy of the X-rays produced. X-rays with higher energy can penetrate deeper into the phantom, thereby increasing the radiation deposits in body organs [20].

The MTF curve in Fig. 4 represents high-contrast spatial resolution [21, 22]. In this study, the choice of low mA or low kV did not significantly affect the high-contrast spatial resolution of the image ($P > 0.05$). However, the low-kV protocol provided a higher MTF curve when applying FBP and IR reconstruction. MTF10% is the threshold for an object that can be observed visually. In this study, MTF10% was always smaller when applying the IR algorithm reconstruction. Another study reported that the spatial resolution of images decreased when using the IR algorithm [23], which is consistent with the results of this study. Thus, reconstruction using standard algorithms, such as FBP, is more effective in detecting lesions with high contrast.

Fig. 5 shows the characterization of the noise in the CT images as a function of spatial frequency. In addition to spatial resolution at high contrast, image noise is an important factor that can affect CT image quality. Reducing noise improves the detection of low contrast in CT images. This study found peak noise in the low-kV protocol to be statistically significantly higher than that in the low-mA protocol ($P < 0.05$). The lower X-ray energy when using a low-voltage tube causes increased attenuation; X-ray stochastic fluctuations occur around the mean value, thereby increasing the noise [20]. However, the noise can be suppressed by iterative reconstruction using the iDose algorithm. The iDose corrects CT number measurements with high noise and then spreads the noise into the image space [24]. IR irradiation significantly reduced the NPS peak. This reconstruction was effective for low-contrast object detection. The results of this study are consistent with those of comparative studies on image quality from multiple CT planes using cylindrical image quality phantoms [17, 25].

The scope of this investigation was limited to a single CT scan; an analysis including a wider range of CT scans from different manufacturers may enhance a more comprehensive understanding. Furthermore, this study does not consider reconstruction using kernel filters. The acquisition parameters examined were limited to the tube voltage (kV), tube current (mA), and IR algorithm specifications. Future research should explore different acquisition methods and reconstruction filters to refine the findings of this study.

IV. CONCLUSION

Low-dose CT with low tube voltage generally shows better dose reduction than low tube current. However, the image noise increases. The low-kV protocol combined with the Filtered Back Projection reconstruction algorithm results in a high increase in spatial resolution, making it suitable for high-contrast object detection, whereas the low mA combined with iterative reconstruction contributes to noise reduction, making it suitable for low-contrast object detection.

Acknowledgments

The authors are grateful to the Ministry of Education and Culture for funding this research through the Master's Thesis Research (PTM) (No. 112/E5/PG.02.00.PL/2023), as well as the management of the Simpang Lima Gumul Hospital, Kediri, Indonesia, for permission to conduct the study and collect and analyze data at the Radiology Facility.

[1] Z. T. Al-Sharify, *et al.*, "A critical review on medical imaging techniques (CT and PET scans) in the medical field", IOP Conf Ser Mater Sci Eng, vol. 870, no. 1, p. 012043, Jun. 2020, doi: 10.1088/1757-899X/870/1/012043.

[2] S. Arifah and A. O. Hidayati, "Gambaran Tingkat Pengetahuan Masyarakat Tentang Pemeriksaan Ct Scan Di Condong Catur Yogyakarta", Jurnal Ilmiah Ilmu Keperawatan, vol. 3, pp. 250259, Dec. 2022.

[3] Y. Nagayama, *et al.*, "Radiation dose reduction at pediatric CT: Use of low tube voltage and iterative reconstruction", Radiographics, vol. 38, no. 5, pp. 14211440, Sep. 2018, doi: 10.1148/RG.2018180041.

[4] K. Martini, *et al.*, "Optimization of acquisition parameters for reduced-dose thoracic CT: A phantom study", Diagn Interv Imaging, vol. 101, no. 5, pp. 269279, May 2020, doi: 10.1016/J.DIII.2020.01.012.

[5] J. Greffier, *et al.*, "CT iterative reconstruction algorithms: a task-based image quality assessment", Eur Radiol, vol. 30, no. 1, pp. 487500, Jan. 2020, doi: 10.1007/S00330-019-06359-6.

[6] J. Greffier, *et al.*, "Impact of dose reduction and the use of an advanced model-based iterative reconstruction algorithm on spectral performance of a dual-source CT system: A task-based image quality assessment", Diagn Interv Imaging, vol. 102, no. 78, pp. 405412, Jul. 2021, doi: 10.1016/J.DIII.2021.03.002.

[7] L. N. Fatichah, *et al.*, "Identification of the computed tomography dose index for tube voltage variations in a polyester-resin phantom", Applied Radiation and Isotopes, vol. 192, p. 110605, Feb. 2023, doi: 10.1016/J.APRADISO.2022.110605

[8] Priyanka, R. Kadavigere, and S. Sukumar, "Radiation dose optimization for computed tomography of the head in pediatric

population An experimental phantom study", International Journal of Radiation Research, vol. 20, no. 4, pp. 747751, 2022, doi: 10.52547/IJRR.20.4.3

[9] M. K. Saeed and Y. Almalki, "Assessment of computed tomography radiation doses for paediatric head and chest examinations using paediatric phantoms of three different ages", Radiography, vol. 27, no. 2, pp. 332339, May 2021, doi: 10.1016/J.RADI.2020.09.007.

[10] Endarko, *et al.*, "Teknik Mendesain Dan Fabrikasi Fantom Antropomorfik Toraks Pasca Mastektomi Payudara Kiri Dengan Kelengkapan Organ. Indonesia", Indonesia Patent, vol. P00202102195, 2022.

[11] AAPM, "Pediatric Chest Routine Protocol", Alexandria, Jul. 2017. Accessed: Sep. 12, 2023. [Online]. Available: https://www.aapm.org/pubs/CTProtocols/

[12] N. Tomic, *et al.*, "Characterization of calibration curves and energy dependence GafChromic XR-QA2 model based radiochromic film dosimetry system", Med Phys, vol. 41, no. 6Part1, p. 062105, May 2014, doi: 10.1118/1.4876295.

[13] C. Anam, *et al.*, "Validation of the tail replacement method in MTF calculations using the homogeneous and non-homogeneous edges of a phantom", J Phys Conf Ser, vol. 1248, no. 1, p. 012001, Jun. 2019, doi: 10.1088/1742-6596/1248/1/012001.

[14] C. Anam, *et al.*, "Impact of Iterative Bilateral Filtering on the Noise Power Spectrum of Computed Tomography Images", Algorithms 2022, Vol. 15, Page 374, vol. 15, no. 10, p. 374, Oct. 2022, doi: 10.3390/A15100374.

[15] C. Anam, *et al.*, "IndoQCT", Diponogoro University. Accessed: Oct. 27, 2023. [Online]. Available: https://indosect.com/indoqct/ .

[16] R. Zeng, *et al.*, "Estimating local noise power spectrum from a few FBP-reconstructed CT scans", Med Phys, vol. 43, no. 1, pp. 568582, Jan. 2016, doi: 10.1118/1.4939061.

[17] P. Barca, *et al.*, "A comprehensive assessment of physical image quality of five different scanners for head CT imaging as clinically used at a single hospital centreA phantom study", PLoS One, vol. 16, no. 1, p. e0245374, Jan. 2021, doi: 10.1371/JOURNAL.PONE.0245374.

[18] K. Yamashita, *et al.*, "Direct measurement of radiation exposure dose to individual organs during diagnostic computed tomography examination", Sci Rep, vol. 11, no. 1, p. 5435, Mar. 2021, doi: 10.1038/s41598-021-85060-5.

[19] V. Rajaraman, M. Ponnusamy, and D. Halanaik, "Size specific dose estimate (SSDE) for estimating patient dose from CT used in myocardial perfusion SPECT/CT", Asia Ocean J Nucl Med Biol, vol. 8, no. 1, p. 58, 2020, doi: 10.22038/AOJNMB.2019.40863.1276.

[20] D. Lira, *et al.*, "Tube Potential and CT Radiation Dose Optimization", American Journal of Roentgenology, vol. 204, no. 1, pp. W4W10, Jan. 2015, doi: 10.2214/AJR.14.13281.

[21] T. Higaki, *et al.*, "Deep Learning Reconstruction at CT: Phantom Study of the Image Characteristics", Acad Radiol, vol. 27, no. 1, pp. 8287, Jan. 2020, doi: 10.1016/j.acra.2019.09.008.

[22] T. E. Plautz, *et al.*, "An evaluation of spatial resolution of a prototype proton CT scanner", Med Phys, vol. 43, no. 12, pp. 62916300, Dec. 2016, doi: 10.1118/1.4966028.

[23] H. G. Kim, *et al.*, "Quantitative Analysis of the Effect of Iterative Reconstruction Using a Phantom: Determining the Appropriate Blending Percentage", Yonsei Med J, vol. 56, no. 1, p. 253, 2015, doi: 10.3349/ymj.2015.56.1.253.

[24] E. A. Takahashi, M. D. Kohli, and S. D. Teague, "A Practice Quality Improvement Project: Reducing Dose of Routine Chest CT Imaging in a Busy Clinical Practice", J Digit Imaging, vol. 29, no. 5, pp. 622626, Oct. 2016, doi: 10.1007/S10278-016-9877-X/METRICS.

[25] Y. Li, *et al.*, "A phantom study comparing low-dose CT physical image quality from five different CT scanners", Quant Imaging Med Surg, vol. 12, no. 1, p. 766, Jan. 2022, doi: 10.21037/QIMS-21-245.